Determining the Global Topology of Resonance Surfaces for Periodically Forced Oscillator Families

Richard P. McGehee
School of Mathematics
University of Minnesota
Minneapolis, MN 55455

Bruce B. Peckham
Department of Mathematics and Statistics
University of Minnesota at Duluth
Duluth, Minnesota 55812

1995

Abstract

Maps of the plane can be generated by sampling the flow of periodically forced planar oscillators at the period of forcing. Numerical studies of the bifurcations present in a two-parameter family of such maps, obtained by varying the forcing frequency and amplitude, have revealed a rich structure. Resonance regions in the parameter space, corresponding to maps having periodic orbits of a certain period, are always a part of the bifurcation picture.

Much insight has been gained into the bifurcation structure by viewing resonance regions as projections to the two-dimensional parameter space of "resonance surfaces" from the four-dimensional phase $\times$ parameter space. Here we continue the study of these surfaces by presenting an algorithm to determine their global topology from the bifurcation diagram in the parameter plane and knowledge of generic codimension-one and -two bifurcations.

1 Background: Forced oscillators and resonance surfaces

Differential equations which can be classified as periodically forced planar oscillators are abundant in science and engineering. These oscillators are often studied by doing a bifurcation analysis on the maps generated, as explained in Section 1.1, by sampling the flow at the time period of forcing. As is typical in studies of periodically forced oscillators, we use the frequency of forcing and amplitude of forcing as our two parameters.

Period-q "resonance regions" (also called Arnold tongues, horns, or entrainment regions), defined as the regions of parameter space where the corresponding maps have a period-q orbit, are always a prominent feature of the bifurcation diagrams. In previous studies ([AMKA, 1986] [P1, 1988], [P2, 1990]), it proved useful to consider sets of period-q points in the phase $\times$ parameter space and view the resonance regions as projections of these sets to the parameter space. Because the parameter space is two-dimensional, the period-q sets are two-dimensional manifolds which we call "resonance surfaces."

In this paper, we look specifically at the question of determining the global topology of various period-q resonance surfaces from the bifurcation diagram in the parameter plane. This is similar to the problem of determining the topology of a surface in three dimensions from its shadow on a plane, but the fact that the ambient space is four-dimensional rather than three-dimensional makes the problem more challenging. We rely on the local features of the resonance surfaces, determined by normal forms and universal unfoldings of bifurcations, to arrive at their global topology. We hope that an understanding of the topology of the resonance surfaces and their relationship to corresponding bifurcation diagrams will aid in understanding of the underlying bifurcation theory.

1.1 The periodically forced oscillator model

A standard model of a periodically forced planar oscillator with parameters α (forcing amplitude) and ω (forcing frequency) is given by

$$\frac{d\mathbf{x}}{dt} = \mathbf{V}(\mathbf{x}) + \alpha \mathbf{W}(\mathbf{x}, \omega t) \tag{1}$$

where $\mathbf{x} \in \mathbf{R}^2; \omega, \alpha, t \in \mathbf{R}$; and $\mathbf{W}$ is periodic with period one in its second variable. The vector fields $\mathbf{V}$ and $\mathbf{W}$ are assumed to be smooth. We assume that for $\alpha = 0$ the nonautonomous flow of (1) has a repelling equilibrium point $\mathbf{c}_0$ inside a normally hyperbolic attracting limit cycle C_0 with frequency $\omega_0 > 0$. We call C_0 the *unforced oscillator* and the frequency ω_0 the *natural frequency* of the system. For simplicity we assume that the unforced flow travels counterclockwise around C_0, C_0 is globally attracting except for the repelling equilibrium point c_0, and $\omega > 0$. See Figure 1.

In performing a bifurcation study of (1), it turns out to be more convenient to use ω_0/ω than ω as our first parameter, and to restrict α to $[0, \infty)$, so we define $\mu := (\omega_0/\omega, \alpha) \in (0, \infty) \times [0, \infty)$. We define $\phi_\mu(\mathbf{x}, t)$ to be the flow of (1) satisfying $\phi_\mu(\mathbf{x}, 0) = \mathbf{x}$. We can then reduce the study of (1) to a two-parameter family $\mathbf{f}_\mu$ of diffeomorphisms of the plane by considering time $1/\omega$ maps of the flows:

$$\mathbf{f}_\mu(\mathbf{x}) := \phi_\mu(\mathbf{x}, 1/\omega) \tag{2}$$

We assume that for $\alpha > 0$ the family $\mathbf{f}_\mu$ is *generic* (in the space of smooth two-parameter families of smooth diffeomorphisms of the plane) so that only codimension-one and -two bifurcations need to be considered. (At $\alpha = 0$, $\mathbf{f}_\mu$ is a time $1/\omega$ map of an autonomous flow, which is not generic: restricted to the invariant circle C_0, $\mathbf{f}_{(a,0)}$ is conjugate to a rigid rotation of $\omega_0/\omega = a$ times around the circle; in particular, if ω_0/ω equals the rational number p/q, every point on the circle C_0 is a period-q point.)

1.2 Small forcing amplitude

The normal hyperbolicity of C_0 at $\alpha = 0$ ensures that for small $\alpha > 0$, $\mathbf{f}_\mu$ will continue to have an attracting invariant curve near C_0. Since all recurrence (other than the fixed point which persists from the unforced vector field's repelling equilibrium $\mathbf{c}_0$) must be on this invariant curve, a bifurcation analysis can be made via circle map theory. The assumptions that $\mathbf{f}_\mu$ is a rigid rotation for $\alpha = 0$ and that $\mathbf{f}_\mu$ is generic for $\alpha > 0$ imply that *resonance regions* (horns, tongues), nonoverlapping for small α, generically open into the first quadrant of the parameter plane from every point on the $\alpha = 0$ axis where $\omega_0/\omega = p/q$ is rational ([Ar, 1982], [Ha, 1984]). A period-q resonance region is defined as the set of parameter values for which the corresponding map has a "least-period-q orbit." (The persistence of a period-q orbit implies

a constant ratio of the *response* frequency to the *forcing* frequency ω for the original differential equation in (1). The two frequencies are said to be *entrained* or *locked* or *in resonance*.) See Figure 2 for the low forcing amplitude portion of a single (period-2) resonance region and some phase portraits for the *second* iterate of the map which might correspond to the indicated parameter values.

Inside the "period-q resonance region," the corresponding phase portraits generically include an attracting invariant "circle in resonance" with at least one pair of period-q orbits, one of the pair attracting and one or the pair repelling when restricted to the circle in resonance. Phase portraits B and C of Figure 2 include examples of circles in resonance. The two sides of the period-q resonance region are saddle-node bifurcation curves for the qth iterate of the map. As the parameters are varied to approach a saddle-node curve from inside a period-q resonance region, a pair of orbits coalesces into a single period-q orbit, neutrally stable when restricted to the circle. Outside the period-q resonance region, as in phase portraits A and D of Figure 2, there are no period-q orbits. Except for the number of orbits which exist at points inside the resonance regions, the collection of all resonance horns, one for each rational point on the ω/ω_0 axis, is the complete bifurcation story for small α.

1.3 Higher forcing amplitudes

As we increase the forcing amplitude, the invariant circles which necessarily persist for small forcing amplitude, can, and in many examples do, break apart. Circle map theory is therefore no longer sufficient to explain the bifurcations.

The period-q points whose existence determines the parameter values that are inside a resonance region, however, can persist whether or not the original invariant circle persists. The same is true for the saddle-node bifurcation curves that form the boundaries of the period-q resonance regions for small α. Many researchers, in fact, were able to numerically "continue" to higher forcing amplitude these saddle-node curves ([KT, 1979], [AMKA, 1986], [KAS, 1986], [MSA, 1988], [P1, 1988], [SDCM, 1988], [VR, 1989]). The numerical work leads to some fascinating bifurcation diagrams. One common feature of these bifurcation diagrams is that, at least for $q \geq 3$, the two saddle-node curves which begin as the two sides of a resonance region

almost always come back together at some higher forcing amplitude. As we shall see in our application in Section 2, the compact region of parameter space bounded by the saddle-node curves is often the projection of a compact surface from the phase $\times$ parameter space to the parameter space. We define these surfaces in the next subsection.

1.4 Resonance surfaces

As suggested in [AMKA, 1986], because a period-q resonance region is defined via the existence of period-q points, it turns out to be more natural to consider the sets of period-q points in the four-dimensional phase $\times$ parameter space than just the corresponding set of parameter values. So we make the following definitions:

$$\begin{aligned}\Gamma(q) \;:=\; &\{(\mathbf{x},\mu) \in \mathbf{R}^2 \times ((0,\infty)\times[0,\infty)) :\ \mathbf{x} \text{ is a least period } q \\ &\quad \text{point of } \mathbf{f}_\mu\}\end{aligned}$$

Because the parameter space is two-dimensional, we expect these sets to be two-dimensional manifolds or surfaces. We actually need to take the *closure* of $\Gamma(q)$ to fill in some "missing points" on the corresponding surfaces for $q \geq 2$. (We are using the subspace topology for $\mathbf{R}^2 \times (0,\infty) \times [0,\infty) \subset \mathbf{R}^4$.)

Definition: A **period-q resonance surface** is a component of $\mathrm{cl}(\Gamma(q))$.

Definition: The projection to the parameter plane of a period-q resonance surface is a **period-q resonance region**.

Because we are most interested in the periodic point surfaces which emanate from the "unforced oscillator," as described in the Small Forcing Amplitude subsection above, we make the following definitions as well.

Definition: The p/q resonance surface := *the* period-q resonance surface containing $C_0 \times (p/q, 0), q \geq 2$.

Definition: The projection to the parameter plane of the p/q resonance

surface is the p/q **resonance region**.

Remarks:

1. The definition of p/q resonance surfaces forces p and q to be relatively prime or the rigid rotation of C_0 under $\mathbf{f}_{(p/q,0)}$ would not have *least* period q, as is required for points on a period-q resonance surface.

2. Surfaces can be identified with a generalized rotation number [P2, 1990] instead of merely a period. Among other things, this means that a p/q surface and an r/q surface cannot connect if $p \neq r$.

3. The fact that a period-q surface "continues" from $C_0 \times (p/q, 0)$, as suggested in the definition of the p/q resonance surface, is justified in the Lemma in the following section.

2 Identifying resonance surfaces

2.1 Local topology

The first order of business is to justify that our resonance surfaces are in fact surfaces. This justification comes from a combination of the implicit function theorem and bifurcation theory; we provide a brief outline of the arguments below. See [P2, 1990] for more details.

Note first that all points on a period-q resonance surface (the period-q points *and* any points in their closure) satisfy $\mathbf{F}(\mathbf{x}, \mu) := {\mathbf{f}_\mu}^q(\mathbf{x}) - \mathbf{x} = \mathbf{0}$. The implicit function theorem guarantees that the period-q surface has a unique local continuation whenever the 2×4 Jacobian matrix $D\mathbf{F}(\mathbf{x}, \mu)$ has rank 2. In order to be sure the surface has a local homeomorphic projection to the parameter plane, however, we require the more restrictive condition: the 2×2 Jacobian matrix $D_{\mathbf{x}}\mathbf{F} = D{\mathbf{f}_\mu}^q(\mathbf{x}) - I$ must be nonsingular. This is equivalent to requiring that $D{\mathbf{f}_\mu}^q(\mathbf{x})$ *not* have an eigenvalue of one. Consequently, we define the **period-q resonance surface projection singularities** (singular with respect to projection to the parameter plane), $Z(q)$, as

$$Z(q) := \{(\mathbf{x}, \mu) \in \text{a period-}q \text{ resonance surface} : D_{\mathbf{x}}{\mathbf{f}_\mu}^q(\mathbf{x})$$

$$\text{has an eigenvalue equal to one}\}$$

In the context of dynamical systems, the surface projection singularities are map bifurcation points, most of which have been extensively studied in the literature. We assume that by restricting ourselves to generic periodically forced oscillators, we can restrict our list of possible projection singularities (corresponding to positive forcing amplitudes, at least) to those of codimension-one and -two. The list is even further restricted because the continuity of a "self rotation number," defined in [P2, 1990], allows only fixed points to be added to the least-period-q points by the closure operation in the definition of the resonance surfaces. We then rely on existing normal forms and universal unfoldings to see that the period-q surfaces are manifolds near all relevant codimension-one and -two bifurcation points. We list the universal unfoldings of the relevant bifurcations, and explicit formulas for the local pieces of period-q resonance surfaces, in the Appendix.

Because of the special form at zero forcing amplitude of maps generated by periodically forced oscillators (as described in Section 1.1), these points cannot be treated with generic map bifurcation theory. The implicit function theorem can still be used, however, to ensure that the period-q surfaces extend locally from the "unforced oscillator" to a topological cylinder. Because this result is not as well-known, we state it more formally.

Lemma: Let the family $\mathbf{f}_\mu(\mathbf{x})$ be defined from a periodically forced planar oscillator as in Section 1.1. (This implies $\mathbf{f}_\mu(\mathbf{x})$ is C^∞ as a function from $\mathbf{R}^2\times$ (parameter space) to $\mathbf{R}^2$). Then for each rational $p/q > 0$, the set of all least-period-q points near the unforced oscillator, $C_0 \times (p/q, 0)$, and having $\alpha \geq 0$, is a C^∞ topological cylinder with $C_0 \times (p/q, 0)$ as a boundary component.

Proof: By the assumptions in Section 1.1, $\mathbf{f}_{(p/q,0)}$ restricted to C_0 is conjugate to a rigid rotation by p/q times around C_0. In particular, all points on $C_0 \times (p/q, 0)$ are least-period-q points and satisfy $\mathbf{F}(\mathbf{x}, \mu) := {\mathbf{f}_\mu}^q(\mathbf{x}) - \mathbf{x} = \mathbf{0}$. We make a local change of phase variables near C_0 by choosing a θ variable in $\mathbf{T} := \mathbf{R} \pmod 1$ along C_0 and an r variable in $(1-\epsilon_1, 1+\epsilon_1)$ (for some $\epsilon_1 > 0$) transverse to C_0. Assume C_0 is described by $r = 1$. Let $(R_\mu(r,\theta), \Theta_\mu(r,\theta))$ be the new coordinates of ${\mathbf{f}_\mu}^q(\mathbf{x})$ where (r, θ) are the new coordinates of $\mathbf{x}$. Then $\mathbf{F}(\mathbf{x}, \mu) = \mathbf{0}$ is equivalent to the two scalar equations

$$R_\mu(r,\theta) - r = 0$$

$$\Theta_\mu(r,\theta) - \theta = 0$$

Our assumption that the unforced oscillator was a normally hyperbolic attracting limit cycle implies $\frac{\partial R_\mu(r,\theta)}{\partial r} < 1$ at $(\mu_1, \mu_2, r, \theta) = (p/q, 0, 1, \theta)$ for any θ. The use of ω_0/ω for our first parameter μ_1 implies that $\frac{\partial \Theta_\mu(r,\theta)}{\partial \mu_1} < 0$ at $(\mu_1, \mu_2, r, \theta) = (p/q, 0, 1, \theta)$ for any θ. These two partial derivatives imply, via the implicit function theorem, that solutions to the system of equations $\mathbf{F}(\mathbf{x}, \mu) = \mathbf{0}$ can be locally continued from the unforced oscillator $C_0 \times (p/q, 0)$, parametrized by the forcing amplitude α (i.e., μ_2) and the angular phase variable θ. Since our map was assumed to be C^∞ in both its phase and parameter variables, the implicit function theorem guarantees that the set of least-period-q points near the unforced oscillator is locally a C^∞ two-manifold parametrized by $(\alpha, \theta) \in (-\epsilon, \epsilon) \times \mathbf{T}$, for some small ϵ. By restricting to $\alpha \geq 0$, we are left with the C^∞ cylinder with boundary corresponding to $\alpha = 0$. This boundary is the unforced oscillator $C_0 \times (p/q, 0)$. □

2.2 The algorithm for determining global topology

We now present an algorithm to identify the global topology of an individual p/q resonance surface with $q \geq 2$. The algorithm will be modified only slightly for the fixed point surface. Note that the completion of step 1, determining *all* bifurcations associated with a p/q resonance surface, may be impossible to justify in applications. Assuming step one, however, the remaining steps can be accomplished. We include step 1 in our "algorithm" because in practice, this is the first step one would perform.

1. **Determine the bifurcation diagram** in the parameter space for the period-q resonance surface in question. In practice, this is done by numerically continuing the two period-q saddle-node orbits which project to the left and right side boundaries near the zero-forcing-amplitude tip of the corresponding period-q resonance region. Any other projection singularities which connect to the continuation of the saddle-node curves are also continued. If other components of projection singularities exist on the surface, we usually locate them (or rule out the likelihood of their existence) with additional numerics (computing various "constant α cross sections", for example).

2. **Divide the surface into pieces** by "cutting" the surface along the curves of these singularities. If necessary to ensure each resulting surface piece projects injectively to the parameter plane (it will be necessary for the period-3 surfaces), make additional cuts which are not necessarily along projection singularities. (The number of cuts on the resonance surface corresponding to each bifurcation curve in the parameter plane is determined from bifurcation theory; the number of resulting pieces from the cuts is also determined from bifurcation theory.) "Flatten" each of the surface pieces by projecting into the parameter plane.

3. For each surface piece which emanates from the unforced oscillator $C_0 \times (p/q, 0)$ **add an appropriate part of the unforced oscillator** which the Lemma of Section 2.1 guarantees to be the boundary of the p/q surface.

4. **Label edges** so that pieces which were cut apart can later be glued back in place. (Familiarity with the "local" surface features, determined by local bifurcation theory partially summarized in the Appendix, and by the Lemma in section 2.1, is essential for this identification.)

5. **Reassemble the surface** "in the parameter plane" by rearranging, flipping, and stretching the flat pieces so the identified edges can be reglued.

6. **Identify the topology of the surface.**

2.3 An application

We use for illustration a two-parameter family of maps which can be thought of as a model of a planar oscillator with periodic "impulse" forcing. This model was preferable to using a standard planar oscillator with periodic forcing as in equation (1) because it enabled us to use an explicit formula for the maps, instead of computing each iteration of the map by integrating the differential equation in the form of equation (1) for the time period of forcing. The computational savings of this approach are considerable. Additionally, the model was chosen to guarantee the maps had a unique globally attracting

fixed point for high enough value of a parameter which can be interpreted as the amplitude of forcing. Consequently, all resonance regions eventually terminate as the forcing amplitude increases.

We define our family of maps, $\mathbf{H}_\mu$, as the composition $\mathbf{g}_\alpha \circ \mathbf{h}_{\omega_0}$, where $\mathbf{h}_{\omega_0}$ is defined as the time one map of the (integrable) flow described by

$$\frac{dr}{dt} = \frac{r(1-r^2)}{1+r^2}, \frac{d\theta}{dt} = 2\pi\omega_0 + \frac{1-r^2}{1+r^2}, \omega_0 \in \mathbf{R}$$

and $\mathbf{g}_\alpha \equiv (1-\alpha)((x_1, x_2)-(1,0))+(1,0), \alpha \in [0,1]$. Note that this caricature allows us to vary ω_0/ω by varying ω_0 instead of ω. ($\omega = 1$ for all our maps since we always take the time one map.) Consequently, we can allow the parameter ω_0/ω to take on any real value. The parameter α plays the role of the forcing amplitude.

Guided by the knowledge of the small amplitude of forcing theory, which assures us that a horn-shaped period-q resonance region emanated from each "rational" point on the ω_0/ω axis (of form $(p/q, 0)$), we numerically followed both (saddle-node) sides of each resonance horn for $1 \leq q \leq 5$ and $0 \leq p/q < 1$. When the saddle-node curves intersected other codimension-one bifurcation curves (such as a fixed-point "Hopf" curve or a fixed-point period-doubling curve), we continued these codimension-one curves as well. The result was Figure 3a. An enlargement of a portion of Figure 3a is shown in Figure 3b. We put the word Hopf in quotes because the "Hopf" curve was defined numerically by requiring the product of the eigenvalues of the fixed point to be one. This condition allow the inclusion of three segments of our "Hopf" curve in Figure 3a which are actually saddles: between the two pairs of "B" points and the one pair of "A" points.

2.4 Applying the identification algorithm

We now walk through the algorithm for several of the resonance surfaces for our example family of maps.

The $1/5$ resonance surface

1. The two period-5 saddle-node curves which marked the boundary of the period-5 resonance region at small forcing amplitude were continued numerically from the parameter value $(1/5, 0)$. They joined a resonant

Hopf bifurcation (a $\sqrt[5]{1}$ point). This formed the skinny 1/5 resonance region illistrated in Figure 3a. An enlargement including the part of the 1/5 region with the $\sqrt[5]{1}$ point is shown in Figure 3b. Since several "$\alpha =$ constant" cross sections of the 1/5 resonance surface all turned out to be qualitatively like the one shown in Figure 4a, we are convinced that there are no other projection singularities on the 1/5 surface. More specifically, there are exactly ten singularities in the projection of the slice in Figure 4a to the ω_0/ω axis: five corresponding to one period-five saddle-node orbit (all having a common parameter value on the left side of the 1/5 resonance region) and five corresponding to another period-five saddle-node orbit (all having a common parameter value on the right side of the 1/5 resonance region).

2. Because a pair of period-5 orbits is born as the parameters are varied from outside to inside the 1/5 resonance region by crossing the saddle-node boundary curve, there are ten saddle-node cuts to be made on the 1/5 surface: five projecting to the left side of the 1/5 region and five projecting the the right side. This results in ten pieces of the 1/5 surface.

3. We add a boundary piece at the "bottom" of each of the ten pieces. The ten boundary pieces make up the unforced oscillator $C_0 \times (1/5, 0)$. This gives us the shape of the ten pieces we start with in Figure 5a. We have labelled the surfaces with "S" or "N," according to whether they are saddles or nodes in the corresponding phase portraits for small forcing amplitudes, although that designation is not necessarily constant on the whole piece.

   Technical Note: Adding the boundary piece to get the shapes of the ten surface pieces in Figure 5a suggests that as we follow a saddle-node curve in the phase $\times$ parameter space with parameter values approaching the tip, $(p/q, 0)$, the corresponding phase coordinates approach a fixed phase point on C_0. This limiting behavior *is* suggested by our numerical studies (not presented here) and we believe it to be generic. In any case, the Lemma in Section 2.1 justifies the topology of Figure 5a, even if the saddle-node sides of the surface pieces *didn't* limit to a fixed phase point as the parameters approached the tip.

4. The edge identifications near the $\sqrt[5]{1}$ point and the fact that the ten

saddle-node curves on the 1/5 surface come together at the $\sqrt[5]{1}$ point are justified by the local bifurcation analysis of a $\sqrt[5]{1}$ point" [Ar, 1982]. The "cyclic" identification of the saddle and node pieces is corroborated by our cross section of Figure 4a and by the fact that the given identifications join the ten added boundary pieces to make a single topological circle. After filling in some details, it is also corroborated by the formula in the Appendix for the period-5 surface near the $\sqrt[5]{1}$ point: a small circle around the origin in the phase space travels back and forth five times across the 1/5 resonance region. For further illustration, we show some projections of a small part of the 1/5 surface near the $\sqrt[5]{1}$ point in Figure 4b.

5. Reassemble as indicated in the rest of Figure 5a.

6. The 1/5 resonance surface is a toplogical disk.

The 1/3 **resonance surface**

1. The left-hand side period-3 saddle-node curve which starts from parameter value $(1/3, 0)$ continues up, around, and back down to the right hand side saddle-node curve. No codimension-two points are encountered on the way. An isolated $\sqrt[3]{1}$ point, however, lies inside (in the parameter space) the curve of saddle-nodes. The existence of this isolated surface singularity point is guaranteed by Theorem 2 in [P2, 1990]; we were able to easily locate it because it had to be on the fixed-point Hopf bifurcation curve; that it is an isolated surface singularity is consistent with the unfolding of the $\sqrt[3]{1}$ point in the Appendix. See the enlargement in Figure 3b where it is apparent that the period-three saddle-node curve extends above the Hopf bifurcation curve; again, this is consistent with the unfolding. As with the 1/5 resonance surface, various cross sections convinced us that there are no other projection singularities on the 1/3 surface.

2. Because of the singular point on the interior, it is still possible that after cutting along the three saddle-node curves, the surface pieces don't project injectively to the parameter plane. In fact, guided by the local universal unfolding of the $\sqrt[3]{1}$ point, we know that the period-3 surface near the $\sqrt[3]{1}$ point, whose formula is given in the Appendix,

projects in a 3-1 fashion to a deleted neighborhood (after removing the $\sqrt[3]{1}$ point) of the parameter plane; all period-3 points in the deleted neighborhood of the $\sqrt[3]{1}$ point are saddles. So we make three extra cuts on the saddle surface, all three projecting to the same curve in the parameter space from the $\sqrt[3]{1}$ point to an arbitrarily chosen point on the period-3 saddle-node curve, as indicated in Figure 5b. This leaves us with three "saddle" pieces to accompany the three "node" pieces. All six pieces project to the parameter plane in the "inverted teardrop" shape of the 1/3 resonance region of Figure 3a, the saddle pieces each having an extra cut.

3. Add the six pieces corresponding to the boundary circle in a procedure similar to that for the 1/5 surface.

4. The cyclical identification of saddle pieces to each other along the "extra" cut is justified by the period-3 surface formula near the $\sqrt[3]{1}$ point given in the Appendix: a closed loop on the period-three surface parametrized by a small circle around the origin in the phase plane projects to a loop which travels three times around the $\sqrt[3]{1}$ point in the parameter plane. This forces the rest of the edge labels given in the first step of Figure 5b. As with the 1/5 surface, the labelling is corroborated because the six boundary pieces are joined to form a single topological circle.

5. Reassemble as indicated in the rest of Figure 5b.

6. The 1/3 surface is a topological disk. Notice that, similar to the 1/5 surface, the $\sqrt[3]{1}$ point can still be thought of as the center of the disk, but, unlike the 1/5 surface, the saddle-node curves don't meet this point.

The 1/2 **resonance surface**

1. The period-two saddle-node curves on the sides of the 1/2 horn for small forcing amplitude each terminate in a degenerate period-doubling bifurcation, where the two points on the period-two orbit come together to form a fixed point. The local bifurcation analysis of such a point [PK, 1991] shows a period-doubling curve passing through such a point.

Continuation of this curve reveals that both degenerate period-doubling points turn out to be on the same period-doubling curve, which forms a circle in the parameter space. This give us the "ice cream cone" shape for the 1/2 resonance region in Figure 3a. As for our other surfaces, additional cross sections convinced us that there are no more projection singularities on the 1/2 surface.

2. After cutting along the saddle-node curves and the period-doubling curves of the 1/2 surface, we are left with four pieces: two which project to the whole 1/2 resonance region, and two which project only to the bottom triangular "cone" part of the region.

3. Add the four pieces corresponding to the boundary circle in a procedure similar to that for the 1/5 surface.

4. The edge identifications are forced by the local bifurcation analysis of the degenerate period-doubling points, where all four surfaces come together, and by the fact that the four added boundary pieces must form a single topological circle. Which pieces are labelled saddles and which are labelled nodes can be determined from corresponding phase portraits, but this does not affect the topology. This is the starting point of Figure 5c.

5. Reassemble as indicated in the rest of Figure 5c.

6. The surface is a mobius strip!! Note that the period-doubling circle is a "generator" of the mobius strip.

The fixed point resonance surface

1. The continuation of the two saddle-node curves which emanate from $(p/1, 0)$ in the parameter plane for any integer p results in a triangular region in the parameter space. Triangles for $p = 0$ and $p = 1$ are shown in Figure 3a. The two top "corners" of the $p = 0$ triangle, shown in the enlargement of Figure 3b, are cusp bifurcations. As for the other surfaces, additional numerical cross sections convinced us there are no other fixed point projection singularities.

2. We make cuts along all the saddle-node curves. We note that there are two fixed points born as we enter any one of the triangular regions across a saddle-node bifurcation, but there is a third one which is involved in the cusp bifurcations. Thus there are three fixed points for parameter values inside the triangular regions and one fixed point outside. The "outside" point can be thought of as the continuation of the repelling "center" fixed point which came from the repelling equilibrium point of the original unforced oscillator. For increased clarity, we choose to make three extra cuts on the surface for each triangular region, one corresponding to the parameter values along each (saddle-node) leg of the triangle but for the surface which is not involved in the saddle-node bifurcation. This leaves us with three pieces which cover each triangular region and a single piece which covers the rest of the parameter space $(-\infty, \infty) \times [0, 1]$.

3. For each triangular region, add the two boundary pieces corresponding to the boundary circle to two of the three trianguar surface pieces. (The "center" fixed point is not part of the unforced oscillator, so the boundary pieces are added to the saddle and node pieces only.)

4. We restrict our description and figures to $-1/2 \leq \omega_0/\omega \leq 1/2$, so that we are dealing with only one of the triangular regions. The saddle piece and node piece are identified along the edges corresponding to the two "legs" of the triangle. The local unfolding of the cusp points implies that the saddle-node pairings of the two surface pieces changes at a cusp point. So the identification at the top of the triangle must be between the third piece (the "center" piece) and one of the other two. As can be verified from phase portraits, the saddle piece is the one which pairs with the "center" piece. The surface not involved in the saddle-node bifurcation must be the one identified with the sides of the "hole" in the surface which represents the unique fixed point for parameter values outside the triangle. This provides the starting point for Figure 5d. The dotted lines indicate the continuation of the fixed point surface to $|\omega_0/\omega| > 1/2$. Note also that the "center" piece of fixed points has boundaries at $\alpha = 0$ and $\alpha = 1$, where our caricature's parameter space was cut off. This boundary is unique to the fixed point surface because for all other p/q surfaces boundary components exist

only at $C_0 \times (p/q, 0)$.

5. Reassemble the four pieces as in the rest of Figure 5d.

6. The surface restricted to $-1/2 \leq \omega_0/\omega \leq 1/2$ is an annulus. That is, topologically, each triangular region corresponds to a hole (a boundary component) in the single surface of fixed points. The whole fixed point surface, then, is a strip with an infinite number of holes.

Remarks:

1. Because the normal forms for any $\sqrt[q]{1}$ point with $q \geq 5$ indicate pairings of saddle surfaces and node surfaces analogous to the pairings near a $\sqrt[5]{1}$ point, the strategy to determine the toplogy of surfaces with $q \geq 5$ is analogous to the strategy we used for the 1/5 surface. Likewise, we expect the topology of all period-3 surfaces to be determined as was our 1/3 surface, the topology of all period-2 surfaces to be determined as was our 1/2 surface, and the topology of all fixed-point surfaces to be determined as was our fixed-point surface. Depending on the relative magnitudes of the normal form coefficients A and B (as in the Appendix) near a $\sqrt[4]{1}$ point, the period-4 surfaces could either be like a 1/5 surface, with a $\sqrt[4]{1}$ point connected to the saddle-node curves, or like a 1/3 surface, with the $\sqrt[4]{1}$ point isolated from the other singular points. The 1/4 surface and 3/4 surfaces of our caricature both appear to be of the former variety.

2. Although we have labelled most surfaces with S (respectively N) for saddle (respectively node), it is not necessary that the continuation of these surfaces stay saddles (respectively nodes) in all applications. Period doubling bifurcations could cause a change from one to the other.

3 Comments

This paper deals mainly with the topology of the resonance surfaces, but only hints at the geometry of the surfaces as they are situated in the four-dimensional phase $\times$ parameter space. Work in progress presents much more

of the geometry, including various three-dimensional projections such as Figure 4b (from the four-dimensional phase $\times$ parameter space) of global resonance surfaces which have been numerically computed [MP1, 1994 and to appear]. A better "feel" for the geometry of these surfaces is provided by a movie illustrating these numerically computed surfaces [MP2, 1992]. Better yet is the understanding obtained by using the computer to interactively rotate the surfaces through various three- and four-dimensional projections.

In dealing with other forced oscillator families we note that for $q \geq 3$ the p/q resonance surfaces are generically orientable two-manifolds with one boundary component. Thus they must be disks with some number of handles. So the topology of resonance surfaces for other forced oscillators can differ from ours only in the number of handles it may have. (This statement holds for $q = 2$ as well, if the conjecture that all period-two surfaces are nonorientable is true.) Although we have seen no "natural" example of a forced oscillator family having a handle on any resonance surface, we can construct families having resonance surfaces with handles by transforming the parameter space. Other parameter space diagrams of forced oscillators [SDCM, 1988] appear to have sets of projection singularities more complicated than in our application, but such complications do not correspond to handles; they can be thought of merely as extra folds with respect to projection to the parameter plane. Both these handles and surface "folds" will be treated in future work [MP 1995].

We point out that although this study targets bifurcations for periodically forced oscillator systems, it is really applicable to generic two-parameter families of maps of the plane. Forced oscillator families differ from the generic case only because there is a known starting point: forcing amplitude (α) equals zero. Because the corresponding map behavior at zero forcing amplitude is not generic, the "boundary circles" we described do not occur in generic families of maps. The other "local" descriptions of periodic surfaces, however, still apply. For example, a period-5 resonance surface which is "born" in a Hopf bifurcation at a $\sqrt[5]{1}$ point can "die" at a second such point. This would result in a period-5 surface which would be a topological sphere. This is a typical scenario for resonance horns corresponding to "secondary" Hopf bifurcations as studied in [PFK, to appear].

We also acknowledge that our study is far from the final word on the study of bifurcations of forced oscillator systems. For example, we have said nothing about the global bifurcations (invariant manifold crossings), the relationship

of the resonance surfaces to the global bifurcations, or the relationship of the resonance surfaces to associated phase portraits. A complete bifurcation study doesn't yet exist. See, however, [VR, 1989] and [P1, 1988] for more complete numerical studies of forced oscillator systems, and [ACHM, 1983] for additional bifurcation features which may be present inside any given resonance region.

In addition to providing a philosophical plug for resonance surfaces as more natural building blocks for bifurcation analysis than the bifurcation regions obtained from their projections to the parameter plane, we note that the use of these surfaces may also provide some practical benefits for numerical computation of bifurcation diagrams. For example, it may be easier numerically to locate the saddle-node boundaries of a resonance surface by computing the whole resonance surface than by computing the saddle-node boundaries directly. In order to do so, however, we must first know the topology of the surface, as studied in this paper, so that we may succesfully parametrize it. Our real goal is to extend the same philosophy to the computation of global bifurcations: computing whole surfaces of homoclinic points may turn out to be a more tractable task than computing the curves of homoclinic tangencies that project to the boundaries of homoclinic regions in the parameter space. The further expectation that homoclinic surfaces can be viewed in many contexts as limits of periodic point surfaces is even more motivation for understanding the topology of resonance surfaces as presented in this paper.

Acknowledgements: Discussions over the last several years with D. G. Aronson, G. R. Hall, and R. Moeckel have been instrumental in the development of the ideas presented in this paper. Work was partially supported by NSF grant DMS-9020220. Figures 4a and 4b were obtained with the aid of "geomview," an interactive geometry viewer developed by The Geometry Center, Minneapolis, MN, a Science and Technology Center supported by the National Science Foundation.

4 Appendix

We list below a table of local representation of period-q surfaces (actually the closure of the least-period-q points) which exist in the neighborhood of

the described fixed-point bifurcation.

Bifurcation:	q	Universal unfolding	Period-q Surface	Reference
Saddle-node (ev*=1)	1	$(x,y) \to (x+\epsilon_1 \pm x^2, by)$	$\epsilon_1 = \mp x^2, y=0$	Ar,GH
Cusp (ev*=1 and hod*)	1	$(x,y) \to (\epsilon_1 + (\epsilon_2+1)x \pm x^3, by)$	$\epsilon_1 = -(\epsilon_2 x \pm x^3)$	Ar, GH
Takens-Bogdanov (both ev*=1)	1	$(\dot{x},\dot{y}) = (y, \epsilon_1 + \epsilon_2 y + x^2 \pm xy)$	$\epsilon_1 = -x^2, y=0$	Ar,Bo GH, Ta
Period-doubling (ev*=-1)	2	$(x,y) \to ((\epsilon_1 - 1)x \mp x^3, -ay)$	$\epsilon_1 = \mp x^2, y=0$	Ar,GH
Degenerate period doubling (ev*=-1 and hod*)	2	$(x,y) \to ((\epsilon_1 - 1)x + \epsilon_2 x^3 \pm x^5, -ay)$	$\epsilon_1 = -(\epsilon_2 x^2 \pm x^4), y=0$	PK
Double -1 (both ev*=1)	2	$(\dot{x},\dot{y}) = (y, \epsilon_1 x + 2\epsilon_2 y \pm x^3 - 2x^2 y)$	$\epsilon_1 = \mp x^2, y=0$	Ar, Ta
$\sqrt[q]{1}$ point	3	$\dot{\mathbf{z}} = \epsilon\mathbf{z} + A\mathbf{z}\lvert\mathbf{z}\rvert^2 + B\bar{\mathbf{z}}^2$	$\epsilon = -A\lvert\mathbf{z}\rvert^2 - B\bar{\mathbf{z}}^2/\mathbf{z}$	Ar, Ta
(ev* = $e^{\pm 2\pi i p/q}$)	4	$\dot{\mathbf{z}} = \epsilon\mathbf{z} + A\mathbf{z}\lvert\mathbf{z}\rvert^2 + B\bar{\mathbf{z}}^3$	$\epsilon = -A\lvert\mathbf{z}\rvert^2 - B\bar{\mathbf{z}}^3/\mathbf{z}$	Ar, Ta
	≥ 5	$\dot{\mathbf{z}} = \epsilon\mathbf{z} + \mathbf{z}^2\bar{\mathbf{z}}A(\lvert\mathbf{z}\rvert^2) + B\bar{\mathbf{z}}^{q-1}$	$\epsilon = -\lvert\mathbf{z}\rvert^2 A(\lvert\mathbf{z}\rvert^2) - B\bar{\mathbf{z}}^{q-1}/\mathbf{z}$	Ar, Ta

* ev = eigenvalue(s) of the fixed point, hod = higher order degeneracy

Comments:

1. For the universal unfoldings given as differential equations, the time one map of the differential equation agrees with the q^{th} iterate of the original map (after a coordinate change) up to arbitrarily high order.

2. The period-q surface formulas are determined directly from the universal unfoldings. For $q \geq 2$, the fixed point at the origin of the phase plane must be "divided out" to leave us with a representation of the closure of the least-period-q surface.

References

[Ar, 1982] Arnold V.I., *Geometrical Methods in the Theory of Ordinary Differential Equations*, Springer Verlag, New York.

[AMKA, 1986] Aronson D.G., McGehee R.P., Kevrekidis I.G., Aris R., "Entrainment Regions for Periodically Forced Oscillators," *Phys. Rev. A* **33** (3) 2190-2192.

[ACHM, 1983] Aronson D.G., Chory M.A., Hall G.R., McGehee R.P., "Bifurcations from an invariant circle for two-parameter families of maps of the plane: a computer assisted study," *Comm. Math. Phys.*, **83**, 303-354.

[Bo, 1976] Bogdanov R.I.,"Versal deformation of a singularity of a vector field in the plane in the case of zero eigenvalues," *Trudy Seminara Imeni I. G. Petrovskogo*, Vol. 2, 23-36, 1976. English translation: *Selecta Math. Sovietica*, Vol. 1, No. 4, 389-421.

[GH, 1983] Guckenheimer J and Holmes P *Nonlinear Oscillations, Dynamical Systems and Bifurcations of Vector Fields*, Applied Mathematical Sciences, **42**, Springer Verlag, New York.

[Ha, 1984] Hall G.R., "Resonance Zones in two-parameter families of circle homeomorphisms," *SIAM J. Math. Anal.***15** (6), 1075-1081.

[KT, 1979] Kai T., Tomita K., "Stroboscopic phase portrait of a forced nonlinear oscillator," *Progr. Theor. Phys.*, **61**(1), 54-73.

[KAS, 1986] Kevrekidis I.G., Aris R., Schmidt L.D., "The Stirred Tank Forced," *Chem. Engng Sci.*, **41**(6), 1549-1560.

[MP1, 1994 and to appear] McGehee R. P. and Peckham B. B., "Resonance surfaces for forced oscillators," Geometry Center Research Report GCG70 (1994) and to appear in *Experimental Mathematics*.

[MP2, 1992] McGehee R. P. and Peckham B. B., "Resonance City," a 15 minute VCR movie made at the Geometry Center, Minneapolis, MN. Available on request from the Geometry Center or the authors.

[MP3, 1995] McGehee R. P. and Peckham B. B., "Arnold Flames and Resonance Surface Folds," Geometry Center Research Report GCG84 (1995) and *Int. J. Bif. and Chaos*, Vol. 6, No. 2., 315-336.

[MSA, 1988] McKarnin M., Schmidt L., Aris R., "Forced oscillations of a self-oscillating bimolecular surface reaction model," *Proc. R. Soc. Lond.A*, **417**, 363-388.

[P1, 1988] Peckham B.B.,"The Closing of Resonance Horns for Periodically Forced Oscillators," thesis, University of Minnesota.

[P2, 1990] Peckham, B.B.,"The Necessity of the Hopf Bifurcation for Periodically Forced oscillators with closed resonance regions," *Nonlinearity***(3)** 261-280.

[PK, 1991] Peckham B.B. and Kevrekidis I.G., "Period doubling with higher order degeneracies" *SIAM J. Math. Anal.*, Vol. 22, No. 6, 1552-1574.

[PFK, 1995] Peckham B.B., Frouzakis C.E., and Kevrekidis I.G., "Bananas and Banana Splits: A parametric degeneracy in the Hopf bifurcation for maps," *SIAM J. of Math. Anal.*, Vol. 26, No. 1.

[SDCM, 1988] Schreiber I., Dolnik M., Choc P., Marek M., "Resonance Behaviour in Two-Parameter Families of Periodically Forced Oscillators," *Physics Letters A*,**128, 1.2**, 66-70.

[Ta, 1974] Takens F., "Forced oscillations and bifurcations," *Applications of Global Analysis* Communications of the Mathematical Instituet Rijksuniversiteit Utrecht, Vol. 3, 1-59.

[VR, 1989] Vance W. and Ross J., "A detailed study of a forced chemical oscillator: Arnold Tongues and bifurcation sets," J. Chem. Phys., 91 7654-7670.

5 Figure Captions

1. Phase portrait of the "unforced" oscillator.

2. The low forcing amplitude part of a period-two resonance horn in the parameter space and accompanying phase portraits for the second iterate of the map.

3. (a) Partial parameter space bifurcation diagram:
   A - Double -1 point
   B - Takens-Bogdanov point (double +1 point)
   C - Cusp point
   D - Degenerate period-doubling point
   qth root of one points - Resonant Hopf points
   "Hopf curve" - defined by product of eigenvalues = 1
   Period-doubling curve - defined by an eigenvalue = -1
   All other curves are saddle-node curves defined by an eigenvalue of the qth iterate of the map = 1. (The appropriate value of q is given by the denominator of the label at the bottom tip of the respective resonance regions.)

   (b) Enlargement of a part of Figure 3a.

4. (a) An $\alpha = .38$ cross section of the 1/5 surface.

   (b) The projection of the 1/5 resonance surface near the $\sqrt[5]{1}$ point from the four-dimensional $(x, y, \omega_0/\omega, \alpha)$ space to the three dimensional $(x, \omega_0/\omega, \alpha)$ space and its "shadow," part of the 1/5 resonance region, a further projection to $(\omega_0/\omega, \alpha)$ space. The five curves along the surface "folds" are period-five saddle-node curves; they all project to the left side of the 1/5 resonance region.

5. (a) The 1/5 surface. Lines a_i and b_i are period-five saddle-nodes.

   (b) The 1/3 surface. Lines a_i, b_i, and c_i are period-three saddle-nodes; lines d, e, and f are "extra" cuts.

   (c) The 1/2 surface. Lines a, b, c, and d are period-two saddle-nodes; lines e and f are period doublings.

(d) The fixed-point surface restricted to $-1/2 \leq \omega_0/\omega \leq 1/2$. Lines a, b, and d are saddle-nodes; lines c, e, and f are "extra" cuts.

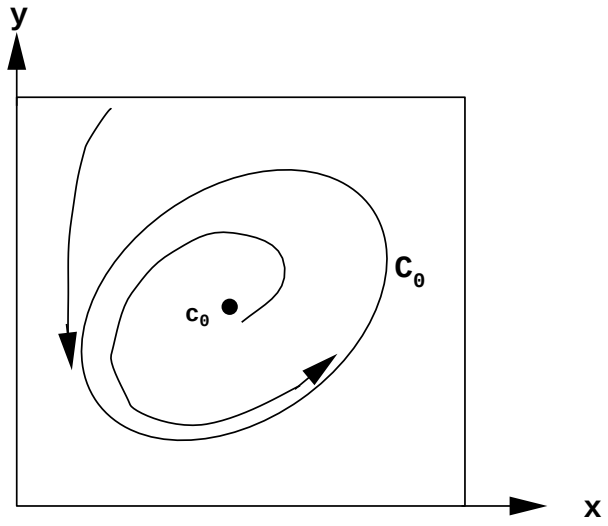

Figure 1

Phase portrait of the ‘unforced’ oscillator.

Figure 1:

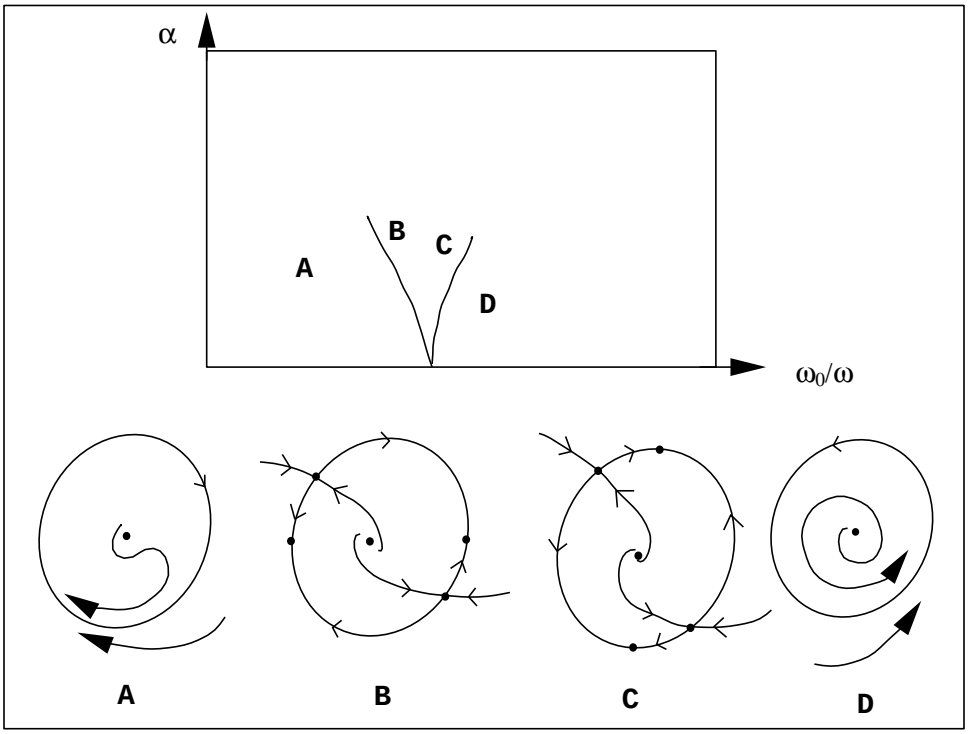

Figure 2

The low forcing amplitude part of a period−two resonance region in the parameter space and accompanying phase portraits for the second iterate of the map.

Figure 2:

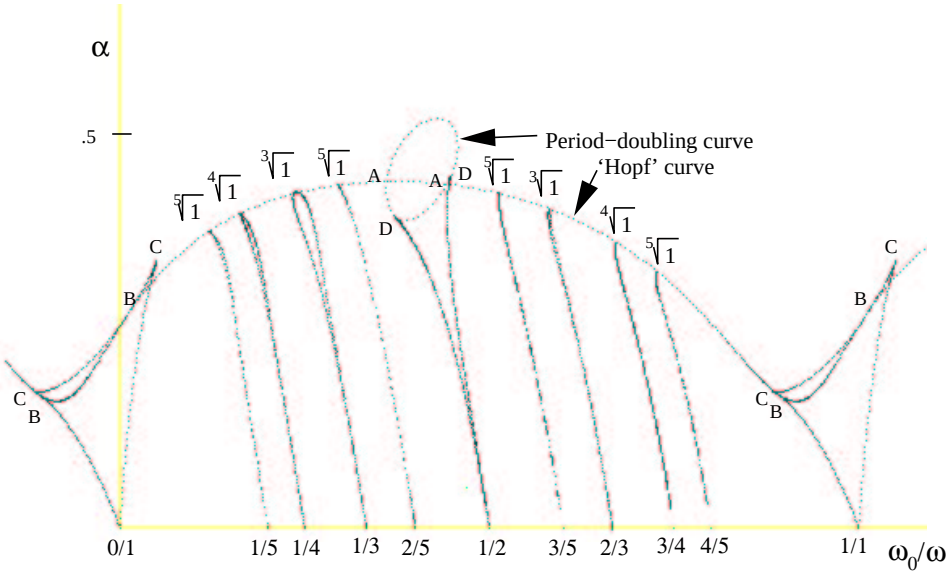

Figure 3a

Partial Parameter Space bifurcation diagram:

A − Double −1 point
B − Takens−Bogdanov point (double +1 point)
C − Cusp point
D − Degenerate period−doubling point
qth root of one points − Resonant Hopf points (eigenvalues qth root of unity)

− 'Hopf curve' − defined by product of eigenvalues = 1
− Period−doubling curve − defined by an eigenvalue = −1
− All other curves are saddle−node curves defined by an eigenvalue of the qth iterate of the map = 1. (The appropriate value of q is given by the denominator of the label at the tip of the respective resonance regions.)

Figure 3:

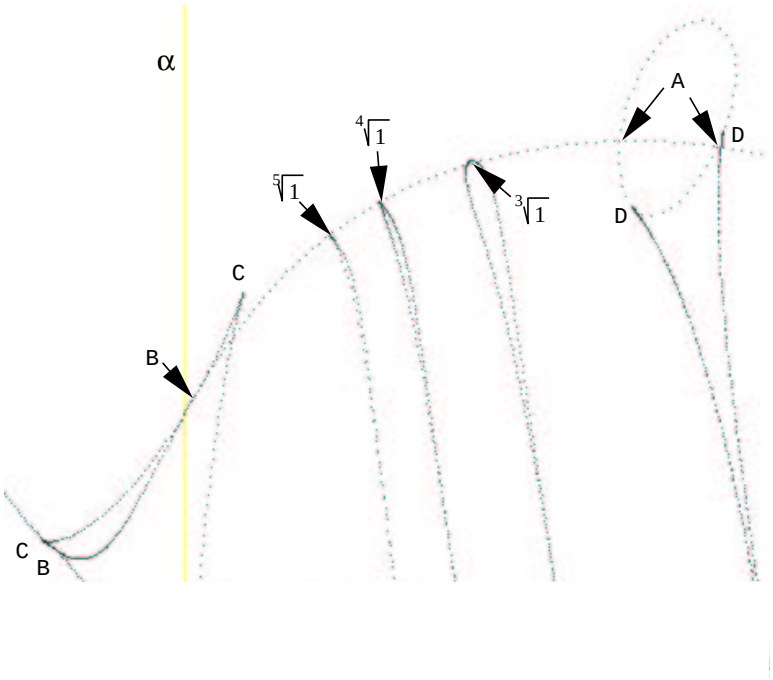

Figure 3b

Enlargement of a part of Figure 3a.

Figure 3:

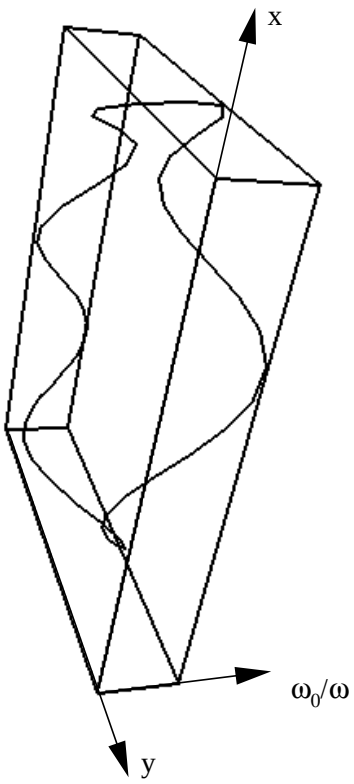

Figure 4a

An $\alpha = .38$ cross section of the 1/5 surface.

Figure 4:

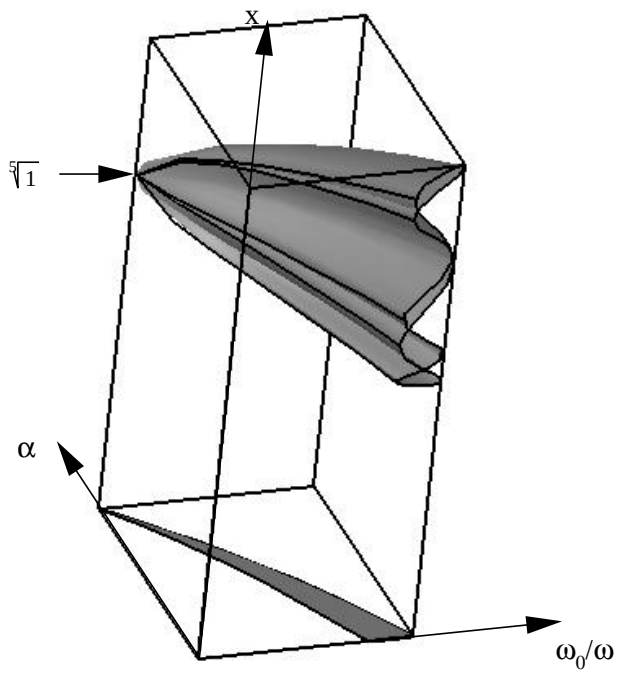

Figure 4b

The projection of the 1/5 resonance surface near the fifth root of one point from the four−dimensional $(x,y,\omega_0/\omega,\alpha)$ space to the three−dimensional $(x,\omega_0/\omega,\alpha)$ and its 'shadow,' part of the 1/5 resonance region, a further projection to the $(\omega_0/\omega,\alpha)$ parameter plane. The five curves along the surface 'folds' are period−five saddle−node curves; they all project to the left side of the 1/5 resonance region.

Figure 4:

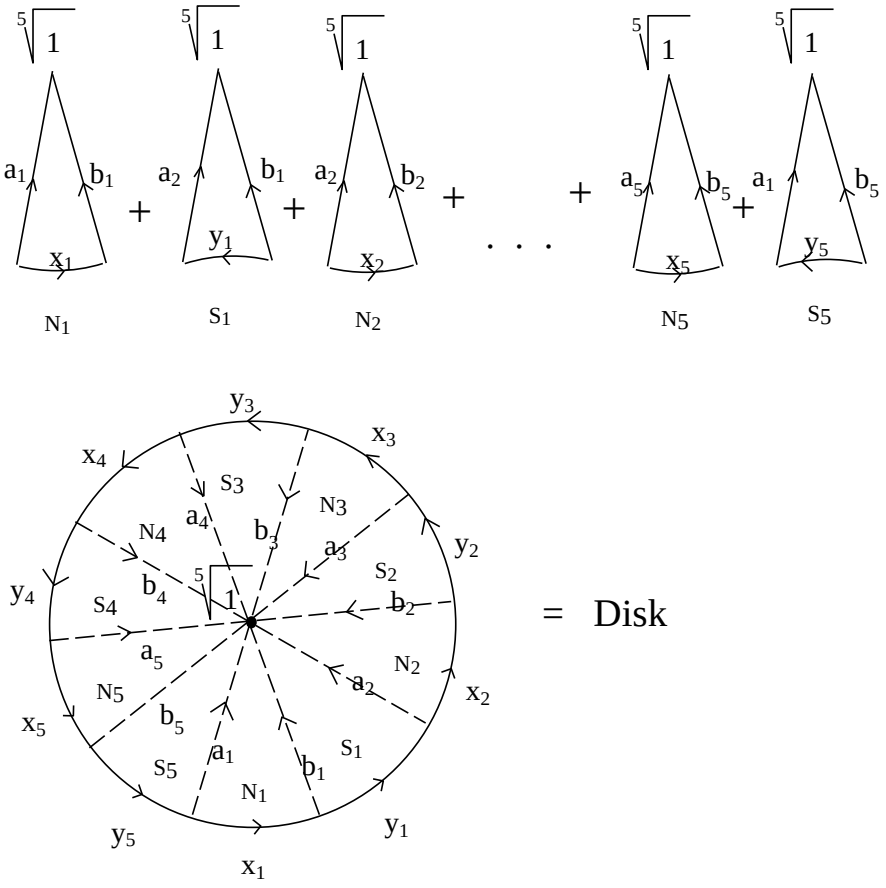

Figure 5a

The 1/5 surface. Lines a_i and b_i are period−five saddle−nodes.

Figure 5:

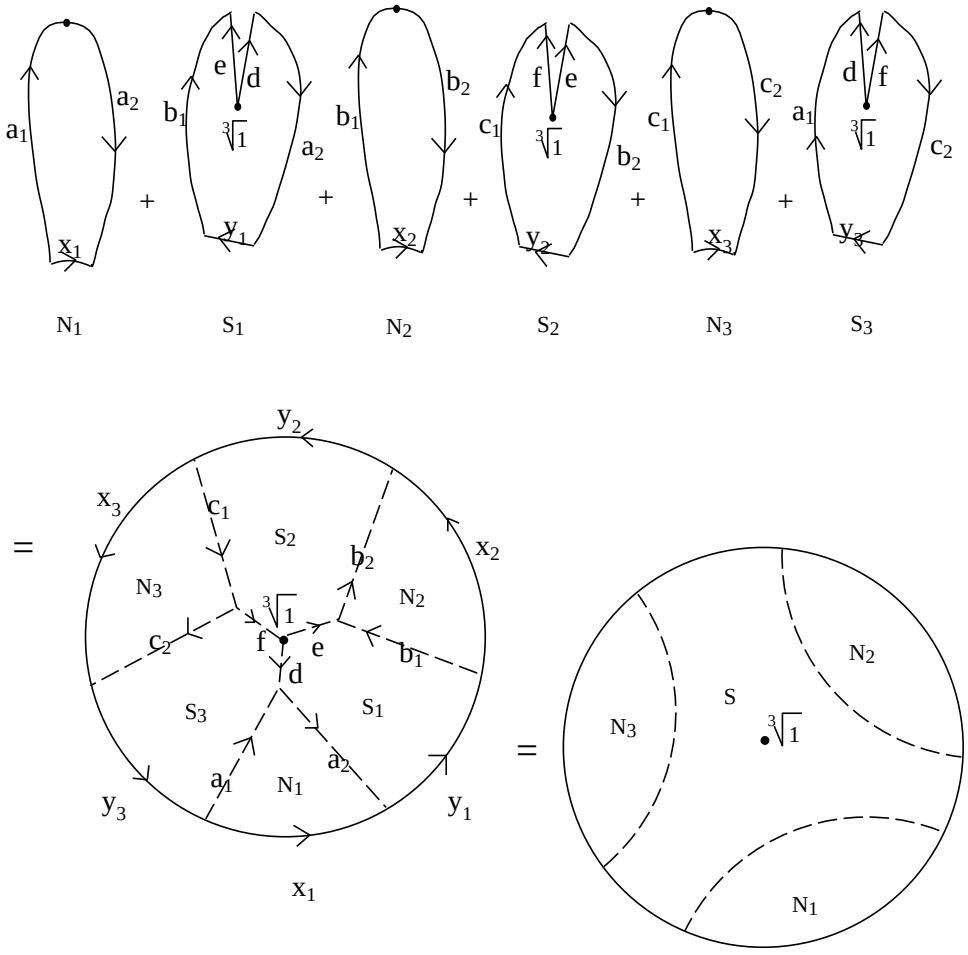

Figure 5b

The 1/3 surface. Lines a_i, b_i, and c_i are period−three saddle−nodes; lines d, e, and f are ‘extra’ cuts.

Figure 5:

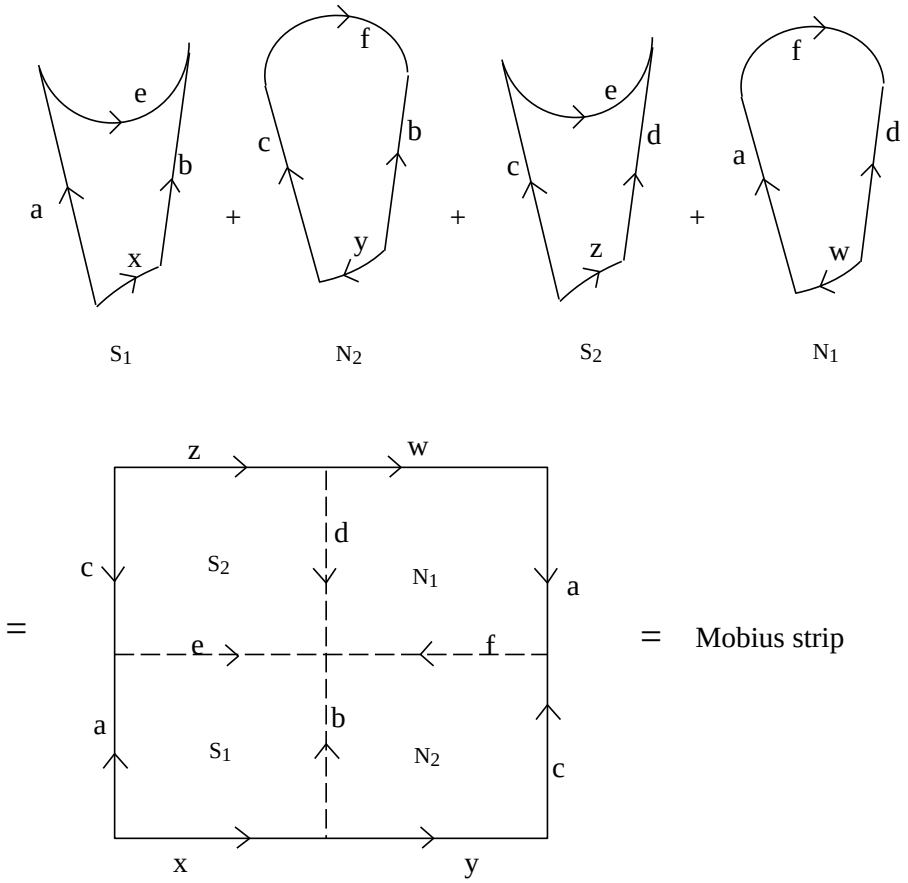

Figure 5c

The 1/2 surface. Lines a, b, c, and d are period−two saddle−nodes; lines e and f are period−doublings.

Figure 5:

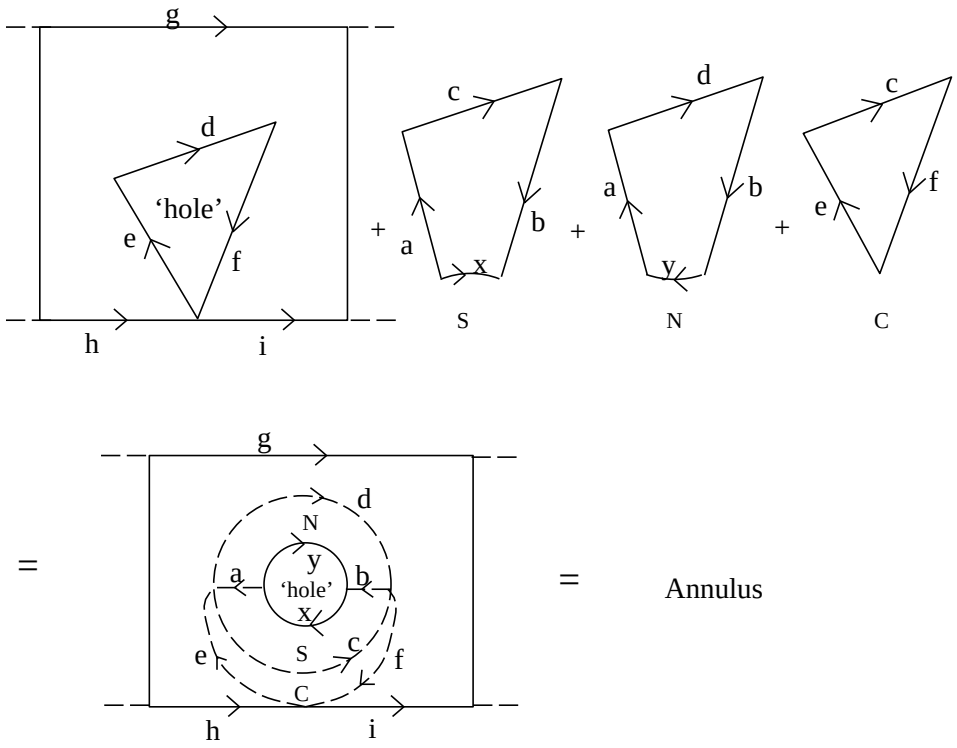

Figure 5d

The fixed point surface restricted to −1/2<=ω<=1/2. Lines a, b, and d are saddle−nodes; lines c, e, and f are 'extra' cuts.

Figure 5: